Safety or not? A Prediction and Programming Model for Submersible Search

Summary

Deep-sea manned submersible is important equipment for entering, exploring, developing and protecting the deep sea. However, the harsh deep-sea environment makes the probability of submersible crash and the difficulty of search greatly increases. At the invitation of MCMS, we build **Submersible Location Prediction Model**, **Evaluation Model for Equipment Preparation** and **Submersible Searching Model** to improve the safety of the submersible.

For Problem 1, we build **Submersible Location Prediction Model**. Firstly, the **configuration of submersible** is set up based on relevant data, and formulas are established to calculate the deep-sea currents, density and seabed depth. Then, the **dynamic analysis** of the submersible in the horizontal and vertical directions is carried out respectively. It is inferred that the weight of the submersible, the direction of the ocean current and the velocity of the ocean current are the important factors affecting the path of the submersible. We use **Monte Carlo method** to simulate the uncertainty of submersible position over time. The uncertainty is constrained by means of unified weighing, water monitoring, measurement of ocean current.

For Problem 2, we combine **TOPSIS and AHP method** to evaluate the equipment preparation. First, we create 11 factors from four perspectives to score and evaluate five powerful search equipment. Considering the difference in function and structure between rescue vessel and host ship, we establish two evaluation systems and use AHP method to calculate the weight of each factor. Based on final score, the rescue vessel is suitable to carry **echo sounder, side scan sonar** and **magnetometer**, while the host ship is suitable to carry **side scan sonar, magnetometer** and **AUV** (autonomous underwater vehicle).

For Problem 3, we draw on the idea of **Dynamic Programming** to optimize search path. First of all, we set the performance of AUV, the device used to submersible search. Then, we define the **maximum density point** as the search target in each time interval. In the two cases of constrained and unconstrained uncertainty, the AUV search path is compared with the possible motion path of the submersible. The special case of staying at the neutral buoyancy point is left to the other carrying equipment to search. Finally, we calculate and plot the probability of finding the submersible that changes over time. It is concluded that the final success probability can reach about 75% and 57% respectively in the two cases, which has high effectiveness.

For Problem 4, we apply our model to the conditions of the Caribbean Sea. It is found that the final probability of search success could reach 98% and about 48% respectively, so the model is highly applicable. Moreover, considering the situation of several submersible moving in the nearby areas, **Multi-submersible Joint Searching Model** is adopted to optimize the search pattern. After analysis and optimization, the success rate of search and rescue can reach 99%.

The sensitivity analysis shows that the success rate of search is still stable at a high level under the condition of changing the search device departure time. We then evaluate the advantages and disadvantages of our model and suggest possible directions for improvement. A memo to the Greek government is attached at the end of our paper.

Keywords: Submersible; Monte Carlo method; TOPSIS; Dynamic Programming

Contents

1 Introduction

1.1 Problem Background

Modern people's understanding of the ocean, especially the deep sea, is far less than that of the land. Deep-sea exploration is to comprehensively study the mysteries of the ocean and the earth, exploring the natural conditions of the deep ocean, such as the appearance of the seabed, ocean currents, as well as the biological and economic resources contained in the seabed. The deep-sea space has complex and special environmental characteristics, its marine meteorology and sea water movement are changeable, and the sea bottom has no light, high pressure, low temperature and no oxygen. The severe Marine environment, equipment failure, human factors and other factors make the deep sea major sudden safety accidents hover at a high level for a long time. In order to reduce the loss of deep-sea accident and find out the cause of the accident, it is necessary to carry out rescue and search and salvage the accident equipment at the first time.

1.2 Restatement of the Problem

According to the requirements of MCMS, we are supposed to support their submersible safety system in the following aspects.
- Develop a model to predict the position of the submersible over time. Through the analysis of uncertain factors, consider the auxiliary positioning information and the corresponding acquisition equipment.
- Under the premise of considering economy and practicality, adding additional search equipment to the main vessel and the rescue vessel.
- By using the information in the positioning model, recommend the initial deployment point and search mode of the equipment in order to minimize the search time, and determine the probability of finding the submersible based on the time and cumulative search results.
- Extend the model to different marine environment and the environment with identified disturbances.
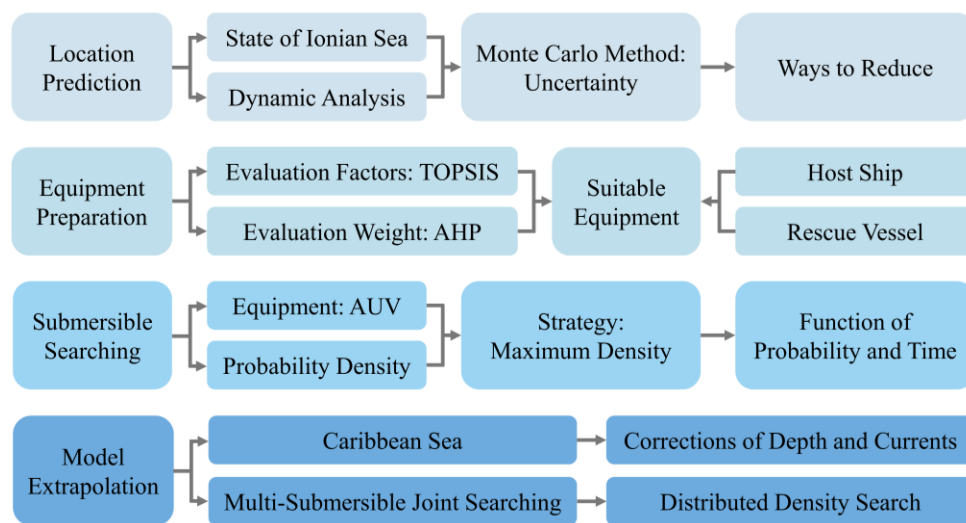
1.3 Our work

Figure 1 Overview of Our Work

2 Assumptions and Justification

We make the following assumptions in this paper:

Assumption 1: We do not consider the rotation of the submersible, that is, only the translational process.

Assumption 2: Communication between submersibles and the host ship is ideal. Before contact is lost, the main ship can receive relevant information from the submersible.

Assumption 3: We do not consider the special weather, such as rainfall, typhoons, etc., and the impact of Marine life on the state of submersible movement.

Assumption 4: In fact, the seabed environment and slope will have an impact on the movement of the submersible. However, to simplify the model, we consider the seafloor topography to be horizontal only because depth affects vertical motion.

Assumption 5: To evaluate safety, our model simulates extreme cases. It is assumed that after the submersible has an incident, it will lose all power. It cannot reach the surface by reducing its mass. The situation that the submersible can automatically rise to the surface is also neglected.

Additional assumptions are made to simplify analysis for individual sections. These assumptions will be discussed at the appropriate locations.

3 Notations

Important notations used in this paper are listed in Table 1.

Table 1 Notations

Symbol	Description	Unit
m	Mass of submersible	kg
$h(t)$	Height of submersible at time t	$minutes$
$v_{sea}(x,y,h)$	Velocity of sea water	m/s
T	Temperature of sea water	$^{\circ}C$
ρ	Density of sea water	kg/m^3
f	Friction between submersible and sea water	N

4   Model I: Submersible Location Prediction Model

4.1 Submersible configuration

In order to simplify the model, through data search and comparison, we set the submersible as a capsule-like shape, and the specific structure and size are shown in the figure below (in meters).
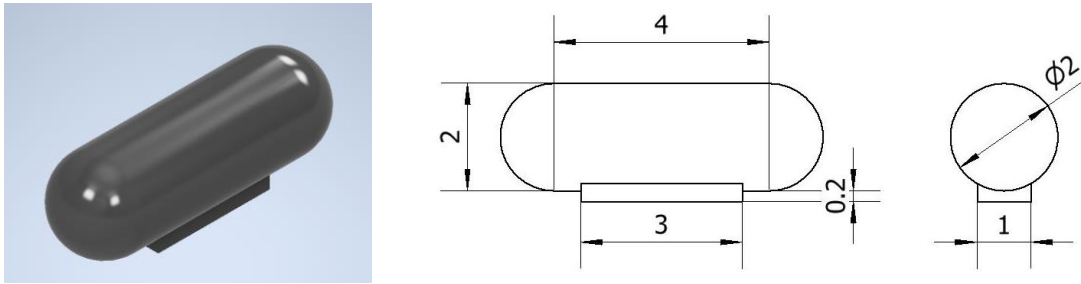

Figure 2 Schematic Diagram of Submarine Model

We can see that the structure of the submersible consists of two parts, the main body of the capsule, and a piece of ballast iron suspended below the body. 压载铁的作用 On this basis, we make further assumptions as follows:

Table 2 Detailed Parameters of Submarine

Length	Width	Height	Full load displacement	Empty Weight	Water Storage Place
6m	2m	2.2m	$16.7552m^3$	$1.0 \times 10^4 kg$	$6m^3$

As a result, the total weight of the submersible m can be expressed as follows：

$$m = m_{empty} + m_{water} + m_{iron} + m_{others}$$

Where m_{empty} is the weight of the empty ship, m_{iron} is the weight of the ballast iron, m_{others} is the weight of other weights such as personnel and equipment, and m_{water} is the weight of water contained in the water storage tank.

4.2 State of the Ionian Sea

The data we use to describe the state of Ionian Sea include historical ocean currents data, density of sea water and the depth of Ionian Sea. The data sources are summarized in Table 3.

Table 3 Data Source Collocation

Database Names	Database Websites	Data Type
HYCOM [1]	https://www.hycom.org/dataserver/gofs-3pt1/analysis	Currents
HURRICAN [2]	https://hurricanescience.org/science/basic/water/index.html	Density
GBECO [3]	https://www.gebco.net/data_and_products	Depth

4.2.1   Currents

Ocean current is a force that cannot be ignored in the ocean, which refers to the regular horizontal flow of sea water in a certain direction at a relatively stable speed, and is the main form of sea water movement. There are three main influencing factors, namely wind, density and compensation. Given the operating area of the submersible, wind and compensation effects have

less effect on ocean currents, and density differences in layers of similar or the same depth are not enough to have large effects. Therefore, we believe that the current data at a certain point tend to be stable as a whole and do not affect the change of seasons over time. On the basis of the above cognition, we obtained the ocean current data at the depth of 4000 meters in the Ionian Sea, and plotted the flow field and velocity characteristic pattern of the ocean current at this depth.
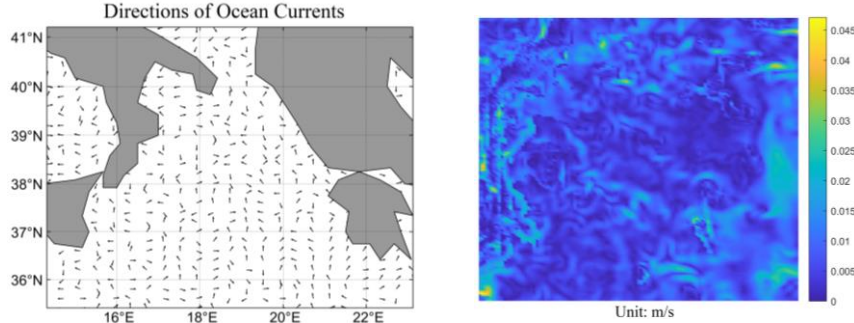

Figure 3 Direction and Value of Ocean Currents in Ionian Sea at $H_0 = 4000m$

From Figure 3, ocean current field in the Ionian Sea is basically disordered in direction, and the remote region still maintains a certain degree of overall direction, while the direction of the ocean current around the land plate is relatively chaotic and does not have overall directivity.

Considering that the search location is in the deep sea, since the ocean current velocity varies with depth and the degree of change is large, the surface current velocity may reach several meters per second, and the deep-sea current velocity is only a few centimeters per second, we use an exponential function to describe the change of ocean current velocity with depth:

$$v_{sea}(x, y, h(t)) = v_{sea}(x, y, H_0) e^{\frac{k(H_0 - h(t))}{H_0}}$$

where $H_0 = 4000m$, $h(t)$ is the current depth, and the constant k can be determined by the sea level current velocity (that is, when $h(t) = 0$).

Since ocean currents are not completely invariable, for the sake of accurate modeling, we determine a velocity magnitude deviation σ in the range of $(-0.3, 0.3)$, so the equation can be further refined as

$$v_{sea}(x, y, h(t)) = (1 + \sigma) v_{sea}(x, y, H_0) e^{\frac{k(H_0 - h(t))}{H_0}}$$

Assuming that the Angle between the ocean current direction and the Y-axis is α, and considering the directional deviation θ of magnitude $(-20°, 20°)$, the value range of the ocean current direction can be expressed as $(\sin(\alpha + \theta), \cos(\alpha + \theta))$.

4.2.2 Density of Sea Water

Through the International one-atmosphere equation of state of seawater (Frank J. Millero, Alain Poisson, 1981) [4], we can determine the density of seawater at the target location, and the equation form is

$$\rho = \rho_0 + As + Bs^{\frac{3}{2}} + Cs^2$$

where s is salinity of water, ρ_0 is density of water, and A, B and C are functions of temperature.

● Temperature

Temperature is an important consideration in the state of the deep-sea environment, and by finding and fitting the data, it is possible to plot the temperature with the depth of the water,

which is also known as thermocline. It can be clearly seen from Figure 4 that the initial temperature decreases significantly with the increase of depth, and then turns to a steady and slow decrease and continues after it drops to 5℃.

● Salinity

Similar to temperature, we perform a similar analysis on seawater salinity to find data for a dataset where a graph of changes can be plotted, which is also known as Halocline. It can be analyzed from the figure that the salinity initially decreases significantly with increasing depth, but after reaching a critical value of about 34.2%, it continues to rise at a lower rate of change than before.

Since salinity and temperature are both known, the corresponding density values can be obtained by calculation, and the data can be fitted to plot the density of seawater with depth.

According to the analysis of the curve trend in the above figure, except for a small decrease near the sea surface, the density increases as a whole with the increase of depth, and the increase rate is large at the shallow layer, and the rate slows down at about 2000 meters.
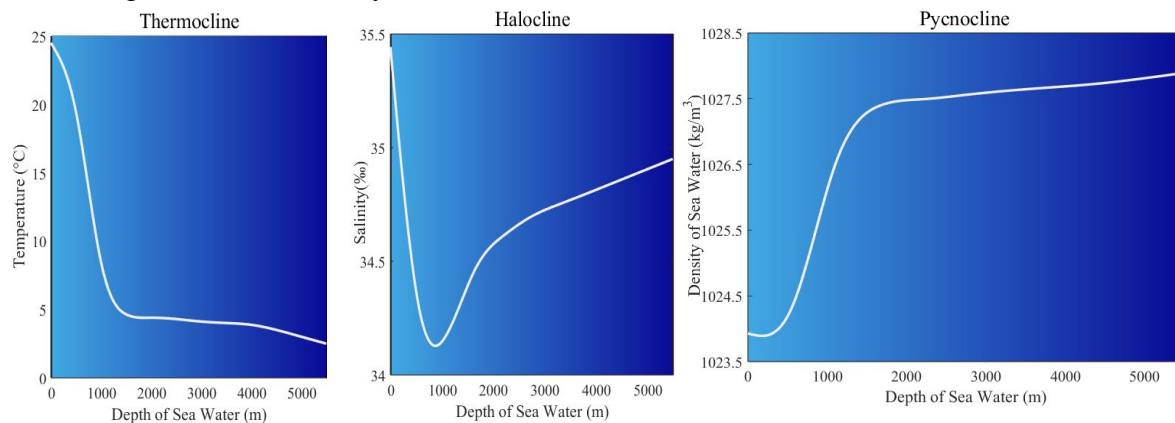

Figure 4 Changes in Seawater Temperature, Salinity, and Density with Depth

4.2.3   Geography of the Sea Floor

The shape of the sea floor is also an important consideration, with fluctuations in the shape of the sea floor determining that the deepest depth can vary from region to region, which in turn can produce different Marine environments. Based on the search data fitting, we have mapped the sea floor characteristic pattern of the Ionian Sea in Figure 5.

Through the analysis of the above figure, it can be seen that the overall depth of the Ionian Sea is basically more than 3000m, and the deepest depth can reach about 5000m. On the whole, compared with other regions, the eastern south region of the Ionian Sea has a deeper seabed.
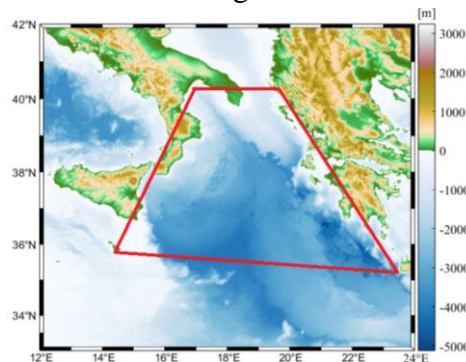

Figure 5 Topographic Map of Ionian Sea

4.3 Dynamic analysis of submersibles

In order to predict the trajectory of the submersible after losing contact and determine the position of the submersible, the dynamics analysis of the submersible is necessary. In order to simplify the model, we assume that the position coordinates of the submersible at the time of crash are $(x, y, h(t))$ and the bow is facing due north.

The force analysis of the submersible is carried out: in the vertical direction, the submersible is mainly subjected to the vertical upward buoyancy F, the vertical downward gravity G, and the resistance f which is opposite to the direction of the submersible's movement relative to the sea water. In the horizontal direction, the submersible is affected only by the resistance f. The diagram is as follows
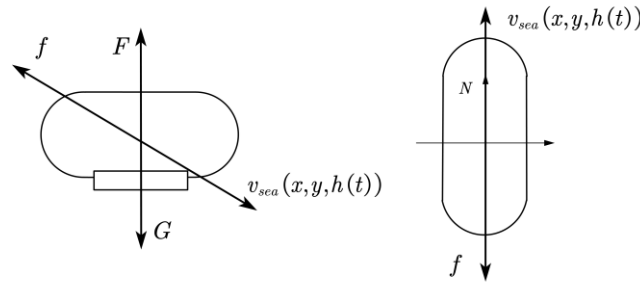

Figure 6 Force Analysis of Submersible

- **Weight:**

$$G = mg$$

where m is the mass of the submersible and $g = 9.8 m/s^2$

- **Floatage:**

$$F = \rho(h) g V_{sub}$$

where $\rho(h)$ is the density of sea water at this depth, and V_{sub} is the volume of submersible.

- **Friction:**

$$f = \frac{1}{2} C \rho S v^2$$

C is the resistance coefficient of seawater, S is the area of the characteristic surface along the axis, ρ is the density of seawater, $v = v_{sea}(x, y, h(t))$. 通过类比，得到潜水器的阻力系数 For the convenience of analysis, the resistance is orthogonal decomposed into the x - and y-axis directions.
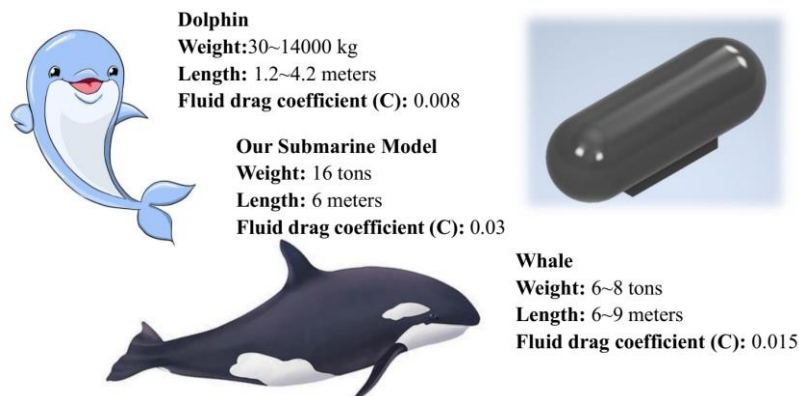

Figure 7 Analogy of Submersible Resistance Coefficient [5][6]

By combining the above three equations, the state equation of the submersible under stress balance can be listed. The considerations and limitations of error in 4.2 are brought into it and can be obtained by comprehensive sorting

$$\begin{cases} m\dfrac{\mathrm{d}^2 h}{\mathrm{d}t^2} = mg - \rho(h)gV_{sub} - \dfrac{1}{2}\rho(h)C_{sub}S_z\left(\dfrac{\mathrm{d}h}{\mathrm{d}t}\right)^2 \\[2mm] m\dfrac{\mathrm{d}^2 x}{\mathrm{d}t^2} = \dfrac{1}{2}\rho(h)C_{sub}S_x\left[v_{sea}(x,y,h(t))\sin(\alpha_{x,y}+\theta_{x,y}) - \dfrac{\mathrm{d}x}{\mathrm{d}t}\right]^2 \\[2mm] m\dfrac{\mathrm{d}^2 x}{\mathrm{d}t^2} = \dfrac{1}{2}\rho(h)C_{sub}S_y\left[v_{sea}(x,y,h(t))\cos(\alpha_{x,y}+\theta_{x,y}) - \dfrac{\mathrm{d}y}{\mathrm{d}t}\right]^2 \\[2mm] h(t) \leqslant H_{sea}(x,y) \\[2mm] \sigma \in (-0.3, 0.3), \theta_{x,y} \in \left(-\dfrac{\pi}{9}, \dfrac{\pi}{9}\right) \end{cases}$$

It can be obtained by analyzing the relationship between the elements expressed in the equation that the randomness of submersible weight, direction and size of ocean currents all affect the position of submersibles. For practical and simplified models, we believe that the submersible will have a completely elastic collision with the seabed when falling to the seabed. In order to verify the rationality of this conclusion, five groups of submersibles with different masses were taken as steps of 0.01kg to simulate the trajectory after the crash. The results are shown in the figure below.
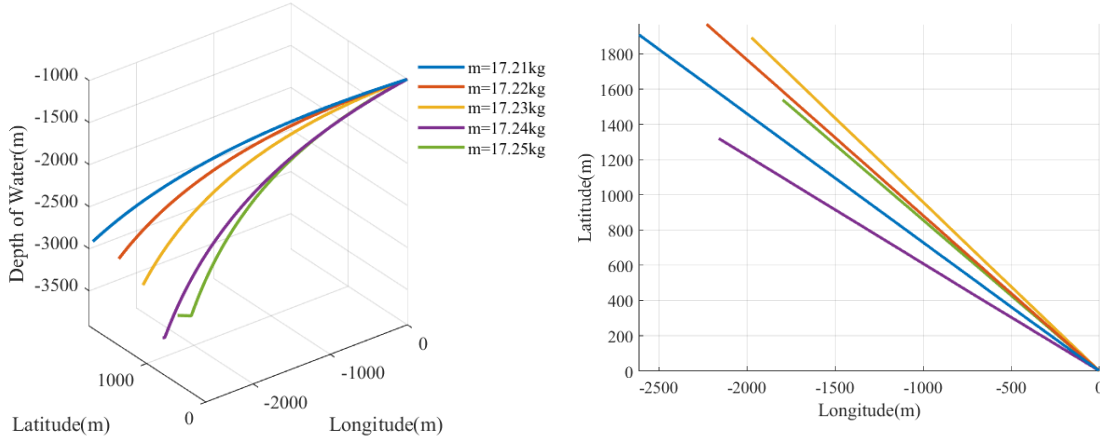

Figure 8 Prediction Location of Submersible over time

From the analysis of the above two figures, it can be seen that even though the mass of the submersible changes only in a subtle range and the deviation between the front and back is very small, the impact on the movement trajectory of the submersible after the crash is indeed significant, which is reflected in the trajectory deviation in the horizontal direction and the distance from the origin, as well as the difference in the falling rate in the vertical direction. In general, when the mass is lighter, the vertical fall rate is slower, which means that the final travel distance in the corresponding horizontal direction may be larger. When the mass is heavier, the vertical fall of the submersible is faster, and the submersible sinks to the sea bottom faster, which means that its displacement in the horizontal direction may be shorter.

4.4 Model Evaluation of Uncertainty

According to the inference in 4.3, the mass of submersible, the direction and size of ocean current are main factors affecting the trajectory of submersible after the wreck, and the uncertainties of the three factors bring more troubles to the position prediction. In order to evaluate the uncertainty, we use Monte Carlo method to simulate the possible position of the submersible.

Monte Carlo method is a method of numerical calculation through a large number of repeated random experiments. Because of its versatility and flexibility, Monte Carlo ideas are often used to solve the following problems: probability distribution statistics, optimization of geometric structures and numerical integration operations. The underwater motion of the wrecked submersible is a stochastic problem, so solving it based on Monte Carlo idea can greatly simplify the calculation model and improve the calculation efficiency and accuracy.

We simulate the possible positions of the submersible at six time points after the accident, and observed the probability distribution of the position of the submersible at that time. The simulation diagram is shown below.
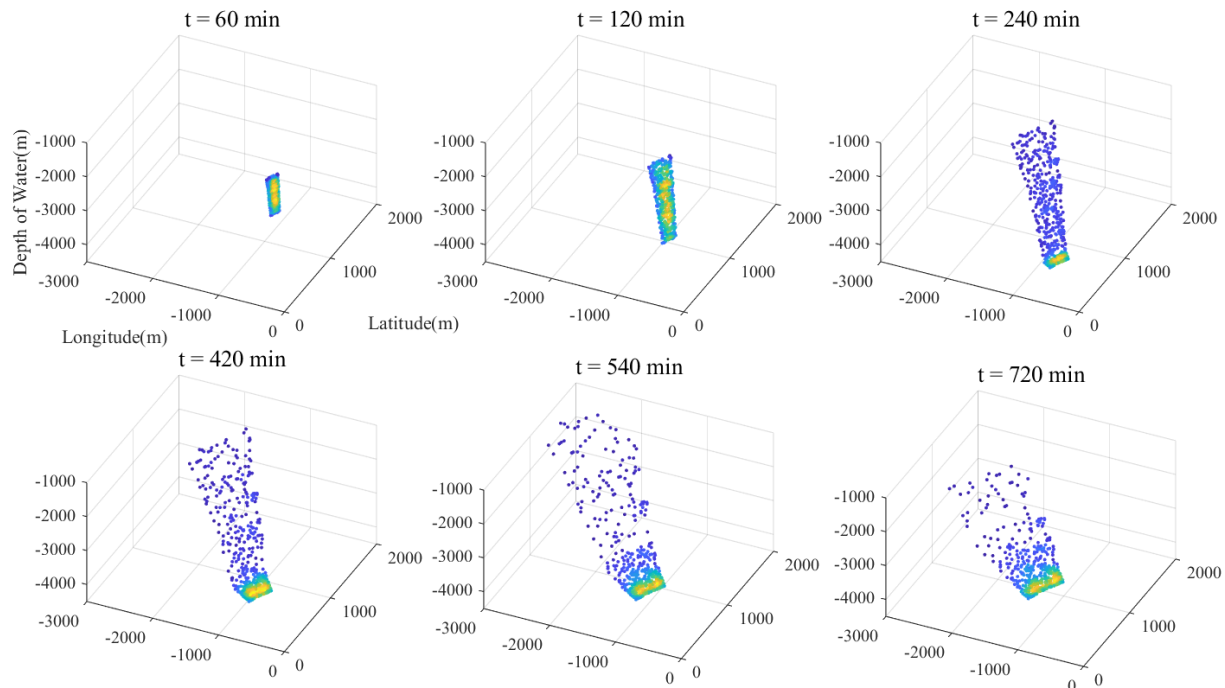

Figure 9 Possible Position of Submersible in Simulation

Through the analysis of the above figure, it can be concluded that with the passage of time, due to the uncertainty of the above three factors at the time of the crash, the probability distribution of the possible position of the submersible has been continuously dispersed over time. In particular, the displacement deviation range in the horizontal direction is too large, which undoubtedly greatly increases the success rate and search and rescue time.

4.5 Ways to Reduce Uncertainty

According to the requirements, the submersible is now considered to periodically transmit some data back to the main ship, in order to reduce uncertainty, help the main ship to conduct more accurate positioning, and facilitate the search and rescue work.

Referring to the inference in 4.3, the uncertainty is mainly concentrated in three aspects: the weight of the submersible, the speed and direction of the ocean current. The instability of the weight mainly comes from the weight of the personnel and equipment carried by the submersible and the weight of the ballast water in the ballast water tank. Therefore, if we can determine the relevant data before the submersible crash, the accuracy of the position judgment of the submersible will be greatly improved. And the following are the equipment and necessary means that we consider suitable for deploying on the submersible.

- Unified weighing before launching to evaluate the **instability of the weight**
- Deploying the instrument monitoring the water quantity in the tank in real time
- Using the water tracking mode of Doppler log DVL to measure the convection velocity, combined with the high-precision navigation parameters provided by SINS self-assisted navigation, using the least squares estimation algorithm RLS to **estimate the ocean current velocity and direction**.

After taking the above measures, the uncertainty about the weight of the submersible and the magnitude and direction of ocean current speeds will decrease. Then, we use 4.4 to build a model to simulate the probability distribution of positions at several time points after the submersible crash.
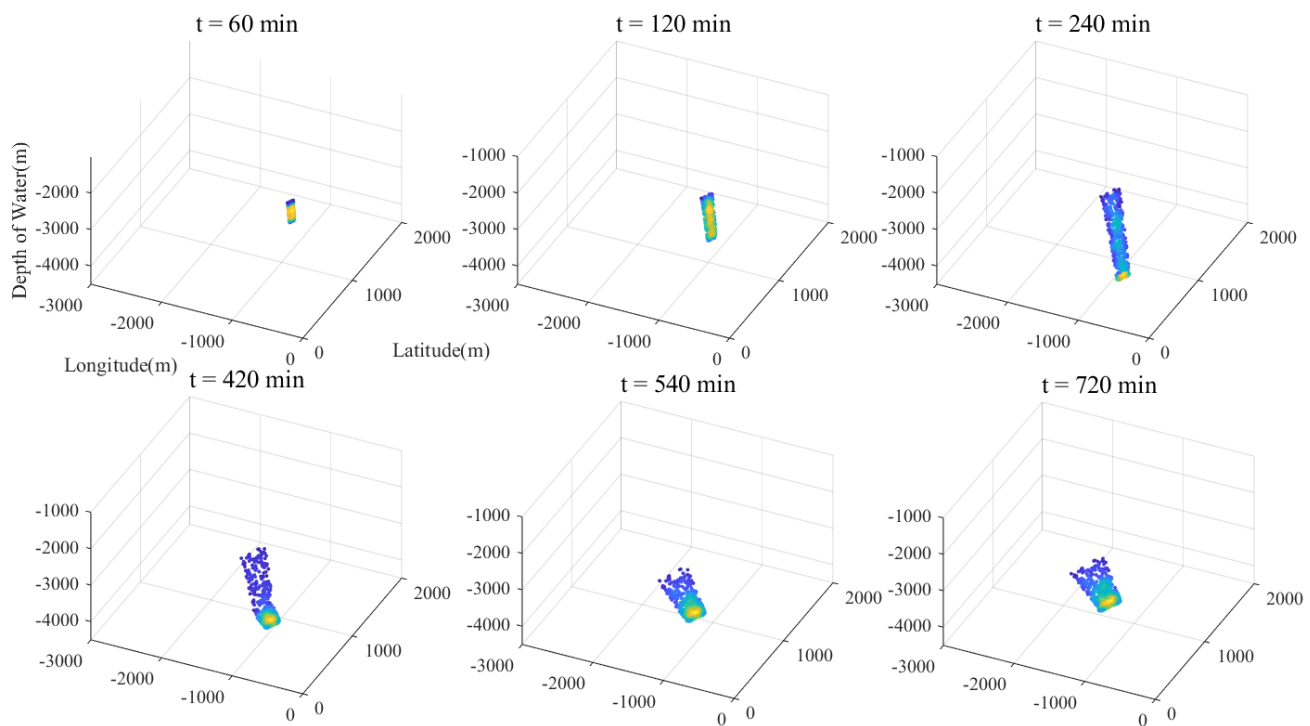
Figure 10 Possible Positions of Submersible with Ways to Reduce Uncertainty

Through comparison and analysis between the above figure and the distribution figure in 4.4, it can be concluded that the probability distribution area for predicting the location of submersible will shrink significantly, and the distribution of random points will be more convergent, which means that the search and rescue area can shrink. **Search time and rescue success rate will be greatly improved.**

5   Evaluation Model for Equipment Preparation

5.1 Evaluation Based on TOPSIS

We are considering installing additional search equipment on the host ship and the rescue vessel, so as to broaden the search means and bring more efficiency to the search and rescue work of the wrecked submersible.

After relevant literature reading and data searching, we select five conventional and powerful medium or large size search and rescue devices: ROV, AUV, Echo Sounder, Side Scan Sonar and Magnetometer, for further evaluation through functional comparison and analysis. The effects, advantages and disadvantages of the equipment are summarized in the following table.

Table 4: Possible Additional Search Equipment

Equipment	AUV	ROV
Effects	Ocean survey, seabed geological research and manned submersible salvage	Remote control operation, seabed survey and deep-sea exploration
Advantages	Autonomous operation, high precision and wide range of action	Multi-functional and continuous working for a long time
Disadvantages	High price, large weight and size	Reliance on cables, limited flexibility, high maintenance costs

Echo Sounder	Side Scan Sonar	Magnetometer
Marine mapping and topographic exploration	Providing a side view of underwater terrain	Find metal objects and locate electronic devices
High precision and efficiency	High definition, wide coverage and strong functionality	No dependence on light, suitable for many environments
Energy Dependence and susceptible to terrain effect	Depth limitation, high investment cost	Low accuracy and may be affected by other metals

For these five devices, we evaluated them using the TOPSIS method. Based on relevant data and subjective thinking, we start from four perspectives and 11 indicators.
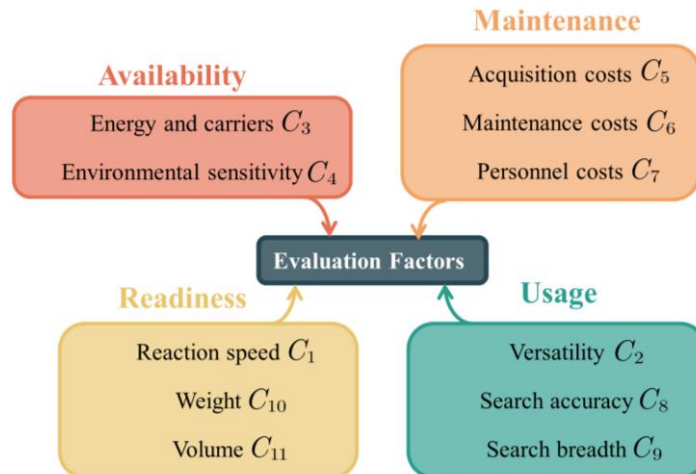

Figure 11 Evaluation Perspectives and Indicators

Refer to the equipment data on the above 11 indicators, and score the five devices respectively. Using the feature normalization method to unify the dimensions of the features can improve the convergence speed and the final accuracy of the model. Therefore, we normalize the data in the quotient table. Standardized evaluation heat maps are shown below.

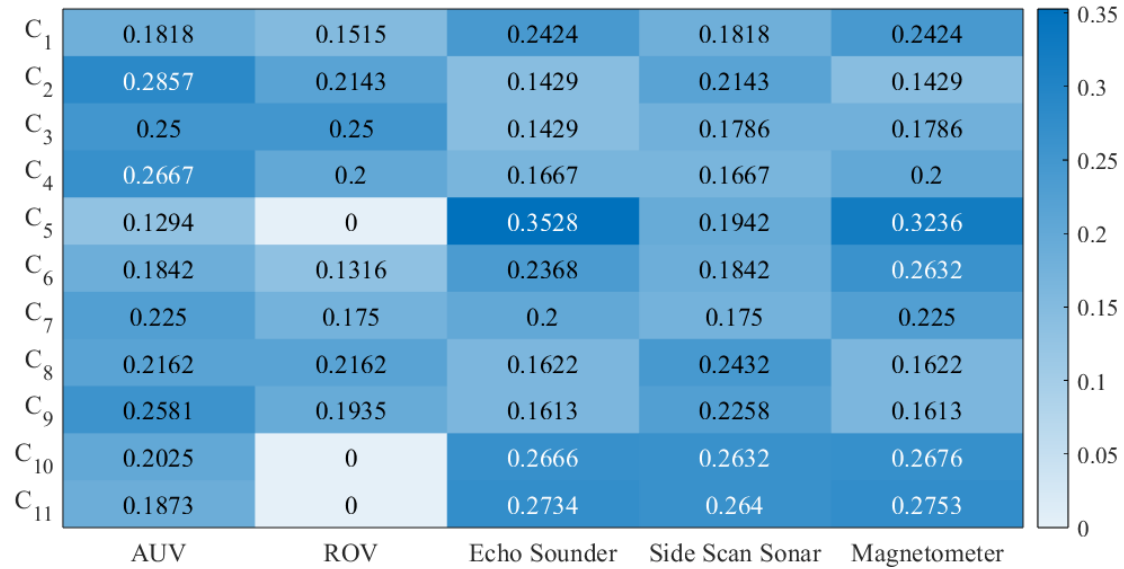|	AUV	ROV	Echo Sounder	Side Scan Sonar	Magnetometer
C_1	0.1818	0.1515	0.2424	0.1818	0.2424
C_2	0.2857	0.2143	0.1429	0.2143	0.1429
C_3	0.25	0.25	0.1429	0.1786	0.1786
C_4	0.2667	0.2	0.1667	0.1667	0.2
C_5	0.1294	0	0.3528	0.1942	0.3236
C_6	0.1842	0.1316	0.2368	0.1842	0.2632
C_7	0.225	0.175	0.2	0.175	0.225
C_8	0.2162	0.2162	0.1622	0.2432	0.1622
C_9	0.2581	0.1935	0.1613	0.2258	0.1613
C_{10}	0.2025	0	0.2666	0.2632	0.2676
C_{11}	0.1873	0	0.2734	0.264	0.2753

Figure 12 Scoring Matrix After Standardization

Considering that different indicators have different priorities in search and rescue tasks, each indicator should have different weights in the evaluation system. Therefore, based on the existing model, we bring in the analytic hierarchy Process (AHP) for further optimization.

5.2 Weight Selection Based on AHP

Analytic Hierarchy Process (AHP) is a decision analysis method that combines qualitative and quantitative analysis to solve complex multi-objective problems. It is necessary to use the experience of decision makers to judge the relative importance of each criterion to measure whether the goal can be achieved. It is more effectively applied to the decision problem with the goal system with hierarchical and staggered evaluation indicators, and the target value is difficult to describe quantitatively

In our model, the host ship and rescue vessel have **a big difference in size and function**: the host ship is larger in the overall space, can carry heavier extra weight, but the moving speed is slower, relatively. The rescue vessel is relatively more flexible, but the space is small and light, the ability of carry is insufficient.

What's more, the rescue vessel should be capable of searching and rescuing people in distress on the surface of the water, towing ships in distress on the far-reaching sea. They can **carry out rescue under harsh sea conditions and complex meteorological conditions**. In view of the differences in the above characteristics, the weights of the evaluation indicators should also be different on the two different ships. AHP is used for the two ships respectively, and the comparison results were represented by heatmaps in Figure 13.

The method of constructing pair comparison judgment matrix can reduce the interference of other factors and objectively reflect the difference of influence of a pair of factors. However, when synthesizing all the results of comparison, it inevitably contains a certain degree of non-consistency. Therefore, it is necessary to check the consistency of the results.
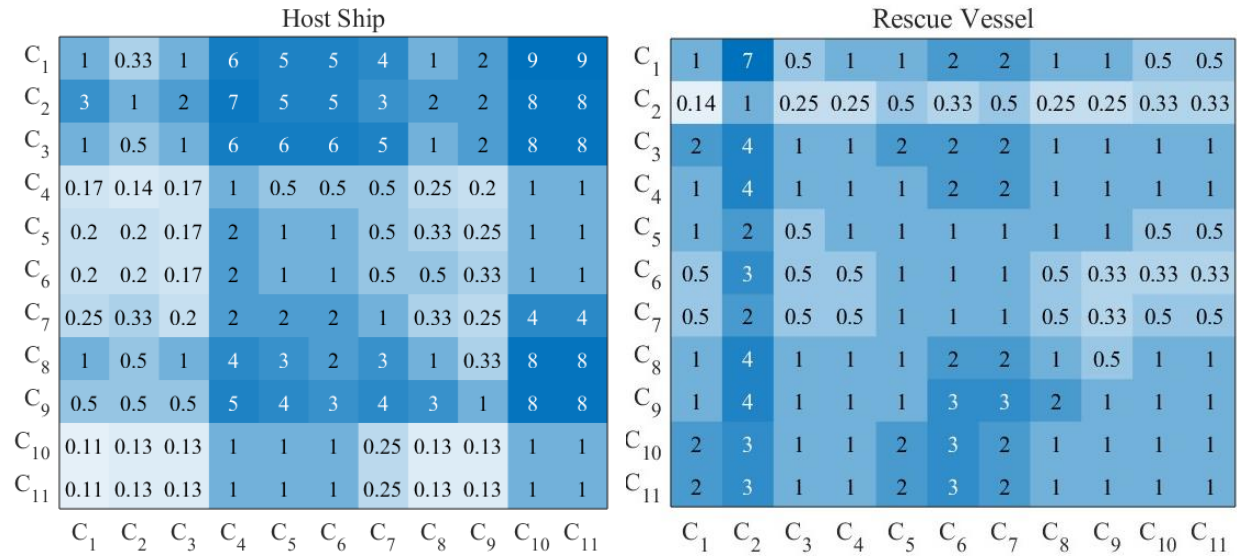
Host Ship

	C₁	C₂	C₃	C₄	C₅	C₆	C₇	C₈	C₉	C₁₀	C₁₁
C_1	1	0.33	1	6	5	5	4	1	2	9	9
C_2	3	1	2	7	5	5	3	2	2	8	8
C_3	1	0.5	1	6	6	6	5	1	2	8	8
C_4	0.17	0.14	0.17	1	0.5	0.5	0.5	0.25	0.2	1	1
C_5	0.2	0.2	0.17	2	1	1	0.5	0.33	0.25	1	1
C_6	0.2	0.2	0.17	2	1	1	0.5	0.5	0.33	1	1
C_7	0.25	0.33	0.2	2	2	2	1	0.33	0.25	4	4
C_8	1	0.5	1	4	3	2	3	1	0.33	8	8
C_9	0.5	0.5	0.5	5	4	3	4	3	1	8	8
C_{10}	0.11	0.13	0.13	1	1	1	0.25	0.13	0.13	1	1
C_{11}	0.11	0.13	0.13	1	1	1	0.25	0.13	0.13	1	1

Rescue Vessel

	C₁	C₂	C₃	C₄	C₅	C₆	C₇	C₈	C₉	C₁₀	C₁₁
C_1	1	7	0.5	1	1	2	2	1	1	0.5	0.5
C_2	0.14	1	0.25	0.25	0.5	0.33	0.5	0.25	0.25	0.33	0.33
C_3	2	4	1	1	2	2	2	1	1	1	1
C_4	1	4	1	1	1	2	2	1	1	1	1
C_5	1	2	0.5	1	1	1	1	1	1	0.5	0.5
C_6	0.5	3	0.5	0.5	1	1	1	0.5	0.33	0.33	0.33
C_7	0.5	2	0.5	0.5	1	1	1	0.5	0.33	0.5	0.5
C_8	1	4	1	1	1	2	2	1	0.5	1	1
C_9	1	4	1	1	1	3	3	2	1	1	1
C_{10}	2	3	1	1	2	3	2	1	1	1	1
C_{11}	2	3	1	1	2	3	2	1	1	1	1

Figure 13 Judgement Matrix of Host Ship and Rescue Vessel

The test requires the following equation to solve the value of the consistency index CR:

$$CI = \frac{\lambda_{max} - n}{n - 1}, \ RI = \frac{\lambda'_{max} - n}{n - 1}, \ CR = \frac{CI}{RI}$$

where λ_{max} is the maximum eigenvalue of the judgment matrix, λ'_{max} is the average value of the maximum eigenvalue, and n is the order of the judgment matrix.

When $CR < 0.10$, it is considered that the consistency of the judgment matrix is acceptable. Otherwise, the judgment matrix should be appropriately modified. Through computational analysis, the CR value of our model is

$$CR_{host} = 0.0345, CR_{rescue} = 0.0237$$

which pass the consistency test and is completely feasible in operation.

Then, we can take the eigenvalue method to solve the weight vector

$$(\omega_1, \omega_2, \cdots, \omega_n)$$

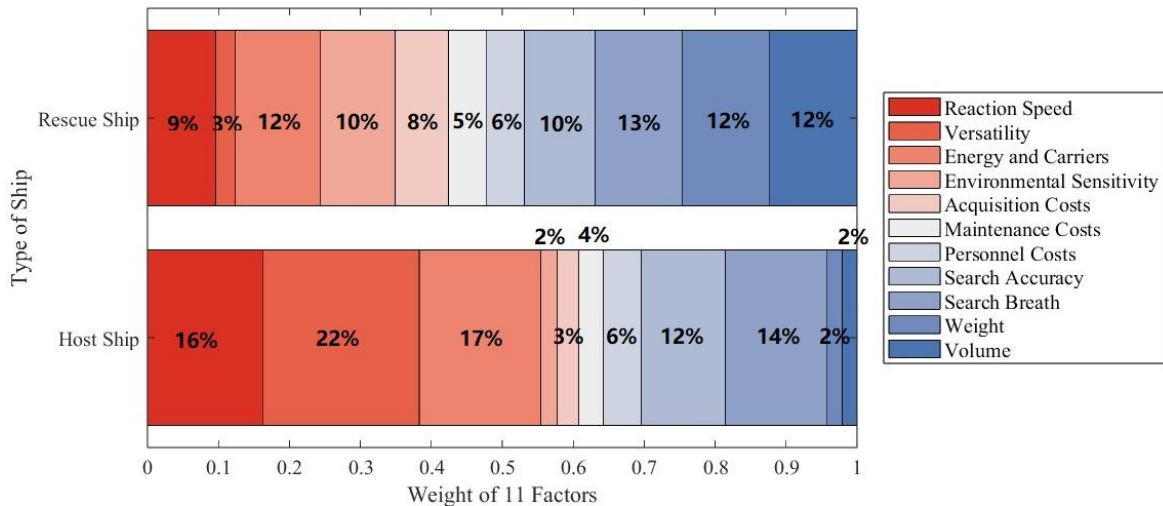where ω_i represents the weight of the $i - th$ factor.

Figure 14 Weight of Each Factors in Different Type of Ship

It can be seen that reaction speed, versatility, energy and carriers occupy a higher priority in the evaluation system of the main ship. Relatively speaking, the evaluation system of rescue vessel is more balanced. It is worth mentioning that due to the small size of the rescue vessel, the weight of the facility volume should be increased.

5.3 Results

For the $i-th\,(i=1,2,...,n)$ evaluation object, the distance between the evaluation objects and the maximum value can be defined as

$$D_i^+ = \sqrt{\sum_{j=1}^m \omega_j \left(Z_j^+ - z_{ij}\right)^2}$$

Where ω_j the weight of the $j-th$ evaluation index.

The distance between the evaluation objects and the minimum value can be defined as

$$D_i^- = \sqrt{\sum_{j=1}^m \omega_j \left(Z_j^- - z_{ij}\right)^2}$$

Then, we can calculate unnormalized scores of each kind of equipment:

$$S_i = \frac{D_i^-}{D_i^+ + D_i^-}$$

Based on the weight distribution in 5.2, calculate the final score of each outfit on two different ships. According to the scoring results of the two evaluation systems, the evaluation radar map is drawn as follows.
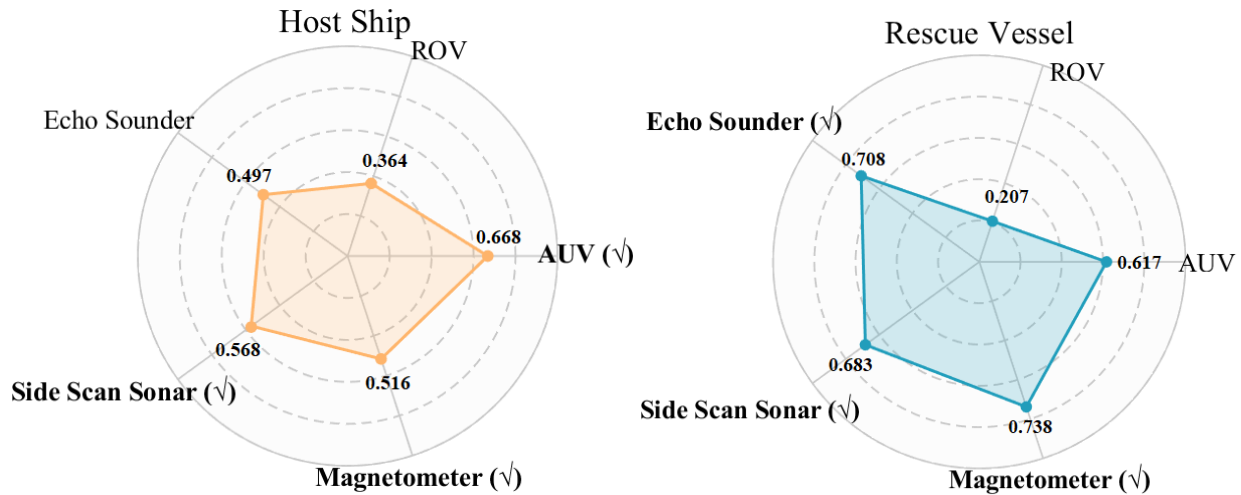
Figure 15 Score of Equipment on Host Ship and Rescue Vessel

The above two figures directly reflect the scores of each device on host ship and rescue vessel. Based on the consideration of many factors such as the space occupied by the devices, energy consumption and maintenance cost, we believe that it is more reasonable for the two ships to carry three devices on each ship.

Therefore, the rescue vessel is recommended to carry **echo sounder, side scan sonar and magnetometer**, and the host ship is suitable to carry **side scan sonar, magnetometer and AUV**.

6 Submersible Searching Model

6.1 AUV's Performance

The AUV, or Autonomous Underwater Vehicle, is a new generation of underwater robots. It can carry a variety of sensors and mission modules, with a wide range of activities, good mobility, safety, intelligence and other advantages, and plays an important role in seabed salvage, Marine research and other aspects. After comparing the data, we decided to use the AUV as the main device for the search and rescue mission. Its structure and performance data are shown below.

Table 5 Performance of AUV

Performance	Battery Time	Maximum endurance speed	Search Radius
Value	8 hours	1.2m/s	20 meters
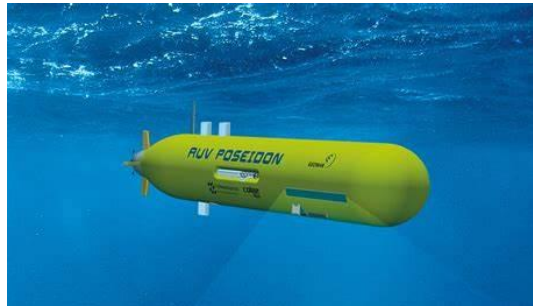
Figure 16 Autonomous Underwater Vehicle (AUV) [7]

6.2 Description of Probability Density

For the moment t, the possible position of submersible can be expressed as

$$S_i(t) = (x_i(t), y_i(t), h_i(t)), \quad i = 1, 2, \cdots, n$$

where n represents the simulation times by Monte Carlo method.

Therefore, we can define the density of point $S_i(t)$ as

$$Den_i(t) = \text{Number of points } S_j(t) \text{ within Radius } R \text{ from } S_i(t)$$

where $j = 1, 2, \cdots, i-1, i+1, \cdots n$ and R is the search radius.

Furthermore, the point with maximum of $Den_i(t)$ can be defined as maximum density point.

6.3 Search Strategy Based on Maximum Density

Set the initial deployment point of the AUV at sea level directly above the impact point and mark that point as the origin point of the coordinate axis. Taking into account the time required for the incident determination, equipment deployment and route planning process, we assumed that the equipment would be put into service two hours after the incident, with the operating time set at 6h to allow time for the device to return.

For any device operating time t, while the device position $P_{AUV}(t)$ is determined at this time, and we perform the following operations:

Step1: Take a certain time interval Δt, calculate all the unexperienced possible positions of the submersible at $t + \Delta t$ and the density of each point, then compare them to get the maximum density point $S_{max\ den}$.

Step2: calculate the function：

$$D(x) = \begin{cases} 1 & when\ v\Delta t \geqslant |P_{AUV}(t) - S_{\max d}| \\ 0 & when\ v\Delta t \leqslant |P_{AUV}(t) - S_{\max d}| \end{cases}$$

- If $D(x) = 1$, drive to the point within this time.
- If $D(x) = 0$, travel the maximum distance with the moving speed of AUV along the connecting line of $P(t)$ and it.
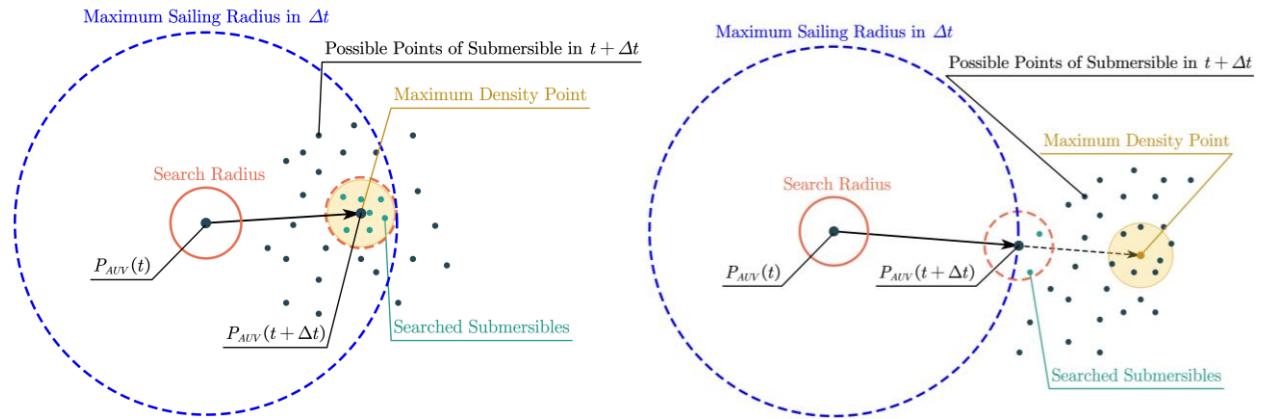
Figure 17 Two Situations in the Searching Process

Step3: Count all the points within the AUV's search radius at $P_{AUV}(t + \Delta t)$ and mark them as submersibles that have been searched.

Step4: Repeat the above steps repeatedly within the time frame until the operating time is reached or the all the submersibles are found.

6.4 Results

Taking into account the timeliness of search and rescue operations, we assume that the AUV deployment time is 2 hours after the submarine loses contact. According to the operation process in 6.3, we can mark the position of the wrecked submersible in each search cycle in the space coordinate system, and draw the approximate search trajectory diagram.

Through the analysis of the above two figures, it can be concluded that the AUV search and rescue route and the possible fall trajectory of the submersible are basically consistent in shape. In addition to the inevitable inconsistencies caused by the distance difference between the initial deployment point and the initial search and rescue position, in the near-seabed space below 3000m, that is, the latter half of the search and rescue process of the underwater vehicle, the search and rescue route and the movement path of the submersible have a very high overlap,

which means that the underwater vehicle search for the crashed submersible is also very likely. It shows a high success rate and efficiency.

Note that the possible path 1 of the submersible in the left figure represents a relatively rare situation, that is, the submersible stays at a **neutral buoyancy point** in the middle of the ocean, so it can be seen that the trajectory curve deviates greatly from the AUV search and rescue route, making the search difficult. In response to this situation, we used echo sounders and side-scan sonar on the main and rescue vessels to assist the search and supplement the model.
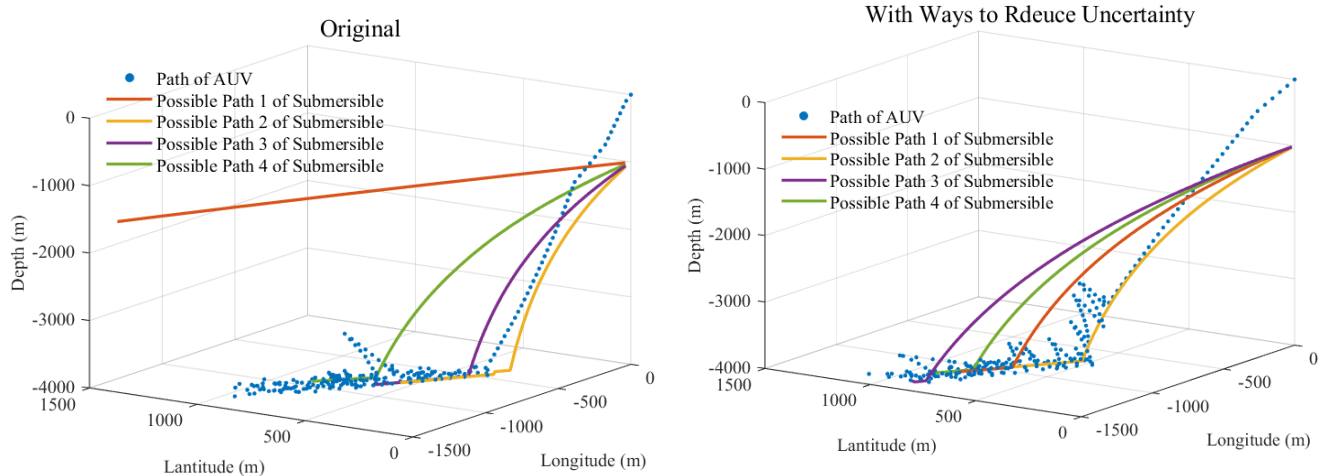
Figure 18 Path of AUV in different situations

In order to verify the effectiveness and success rate of this search strategy, the probability of finding the submersible at different time points is obtained, and the results were fitted in time order to obtain the curve change diagram as follows.
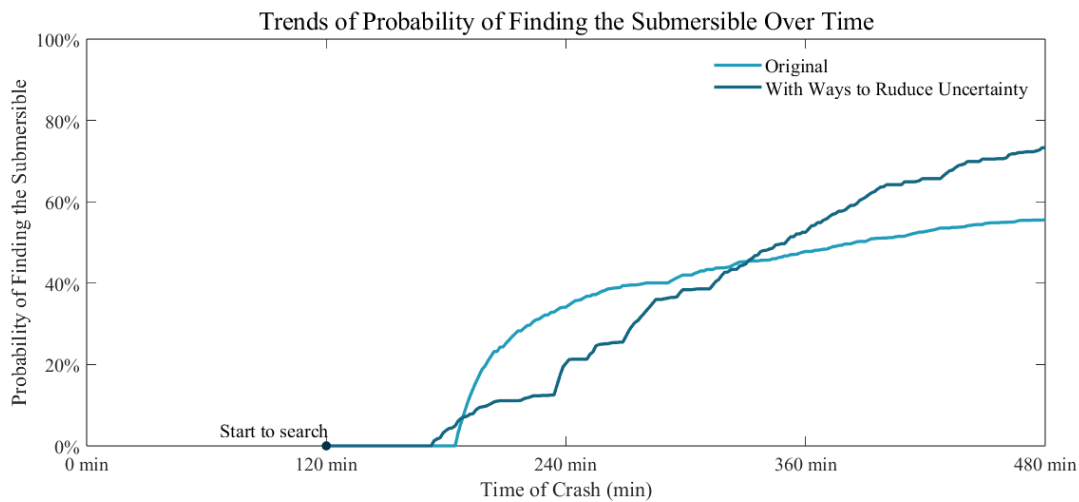

Figure 19 Trends of Probability of Finding the Submersible Over Time

After the search device begin to operate for a period of time, the search success rate begins to gradually climb. In the period of 4-5 hours from the crash time, the probability of success will have several relatively large jumps, and then maintain stable growth. **The final search success rate will reach about 75%.** Considering the fault tolerance ability of the model, if the uncertainty of the location of the crashed submersible is not constrained, the final success rate of search and rescue can still be close to 57%.

7 Model Extrapolation

7.1 Re-discussion in Caribbean Sea

According to the requirements of the topic, the application scope of the model is now considered to extend to other sea areas. Take the Caribbean Sea as an example for analysis, we obtain data from the network, and draw the topographic map.
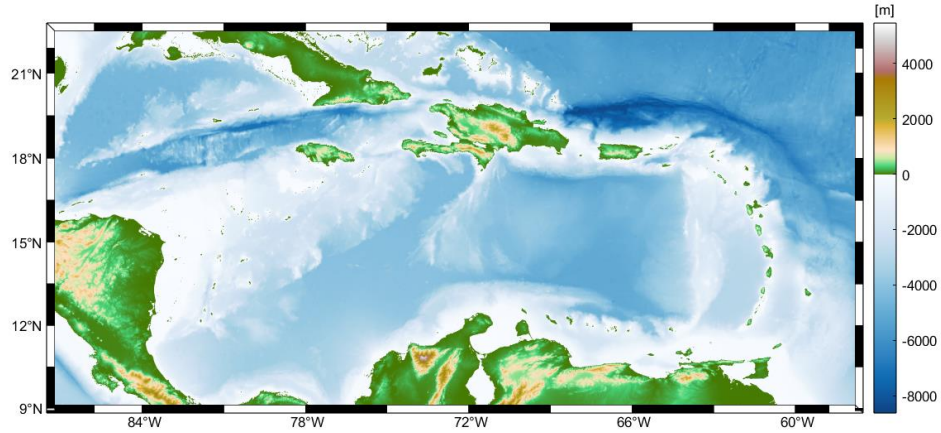

Figure 20 Topographic Map of Caribbean Sea

The comparison between the above figure and the Ionian chart in 4.2.3 shows that the seabed depth of the Caribbean Sea is not much different from that of the Ionian Sea. Since it is surrounded by land, the seabed structure is shallow on all sides and deep in the middle.

After data analysis and relevant information search, we found that the environment of the Caribbean Sea is more severe, and the speed of ocean currents is faster than that of the Ionian Sea. Therefore, we need to make a suitable correction to the ocean velocity v_{sea} in Model 1.

Using the previous model, the Monte Carlo method is used to generate 500 underwater vehicle tracks and search paths under two conditions of constrained uncertainty and unconstrained uncertainty.
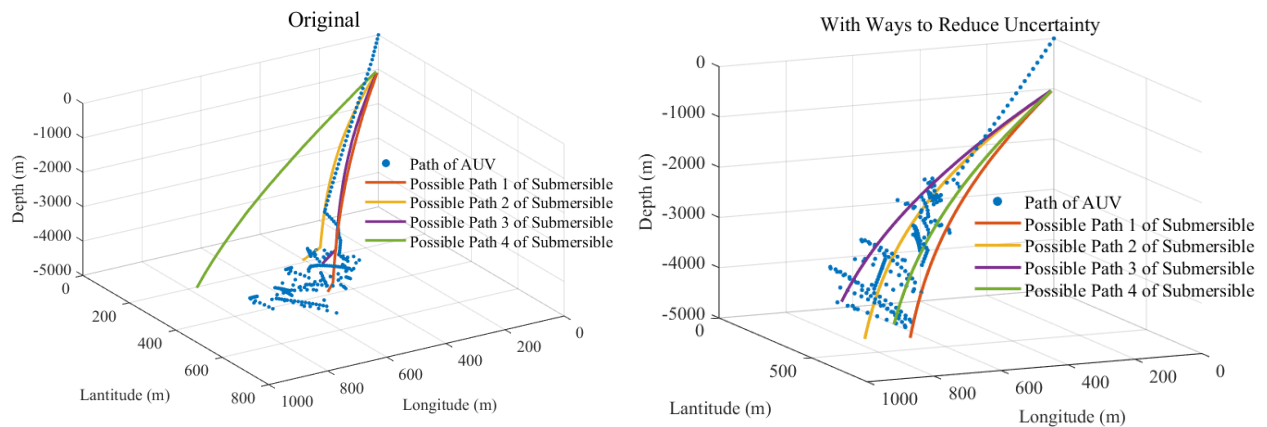

Figure 21 Path of AUV in different Situations

By analyzing Figure 21, it can be seen that the search path and the trajectory of the submersible are still highly coexisting, which indicates that the model is still highly practical under the new conditions.
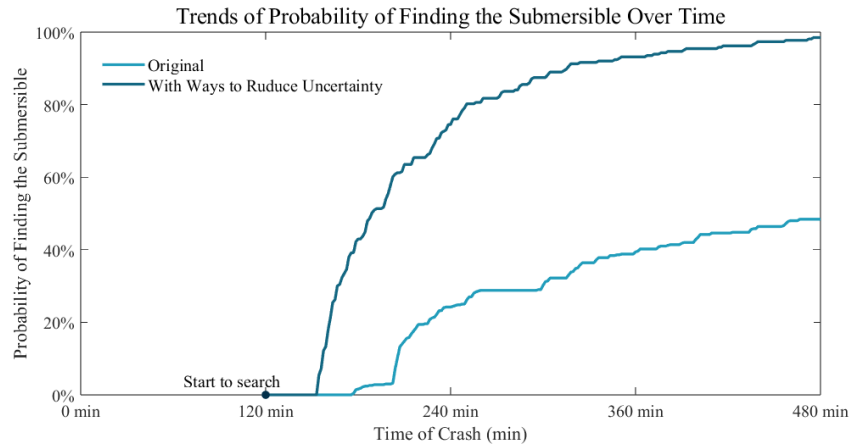

Figure 22 Trends of Probability of Finding the Submersible Over Time

From Figure 22, we find that in the Caribbean Sea, the success rate of our strategy eventually reached an amazing 98%, and even with unconstrained uncertainty, the success rate was still about 48%.

7.2 Multi-submersible Joint Searching

Consider the presence of multiple submersibles in the area. We use three examples for simulation, in which one submersible crashes while the other two submersibles in the area are still intact. We assume that the speed of Submersible 1 and the speed of submersible 2 will be combined into the Submersible Searching Model to participate in search and rescue.

For efficiency reasons, target G is set for the AUV and the submersibles as follows:

$$G_{AUV} = S_{maxden}, \quad G_1 = S_{2/3\,maxden}, \quad G_2 = S_{1/3\,maxden}$$

where $S_{2/3\,maxden}$ indicates to the point that the density is around $2/3$ of maximum density value, $S_{1/3\,maxden}$ indicates to the point that the density is around $1/3$ of maximum density value.

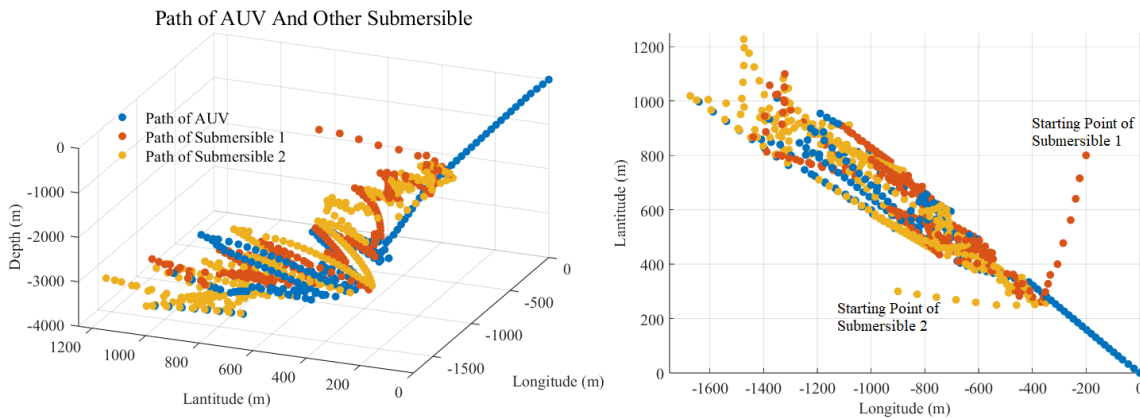Mark the new search trajectory and draw a simulation diagram as follows.

Figure 23 Path of Multi-Submersible Joint Searching

Through the analysis of the figure above, it can be seen that compared with AUV search alone, the addition of two submersibles makes the judgment points become denser, the search coverage is greatly improved, and the AUV route is optimized to a certain extent.

The probability of finding the submersible at each time point is calculated, and the results are fitted to obtain the following curve change diagram
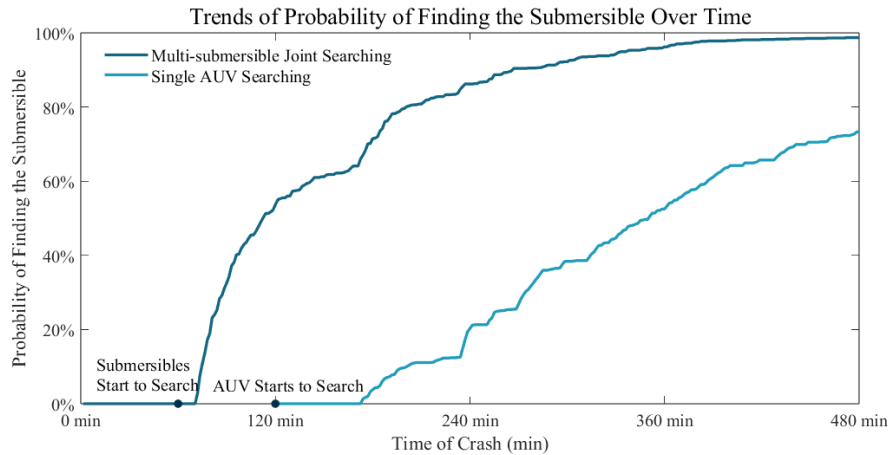

Figure 24 Trends of Probability of Finding the Submersible Over Time

Analysis of the above figure shows that when two submersibles join the search and rescue process, the probability of success in the final search can **reach an astonishing 99%.** Compared to the 75% final success rate shown in 6.4, the results of the new search method are undoubtedly a significant improvement.

8   Sensitivity Analysis

In the Submersible Searching Model, we assume that the departure time of the AUV is fixed to 2 hours. Therefore, we need to conduct sensitivity analysis on this factor.
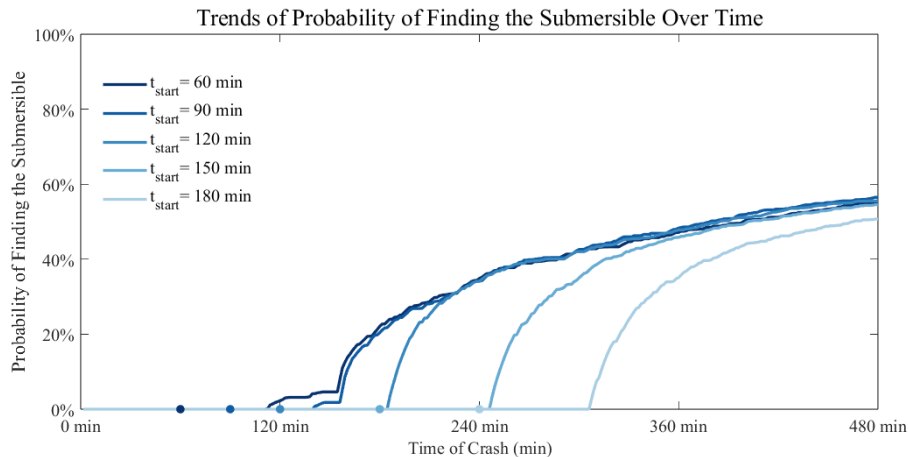

Figure 25 Trends of Probability Over Time in Original Situation

Figure 25 shows the trends of probability over time in situation of unstrained uncertainty. Although the departure time varies from 60 to 180 minutes, the probability of successful search and rescue tends to be stable at $55-60\%$ at the 8th hour after the submersible loses contact, with no obvious change.
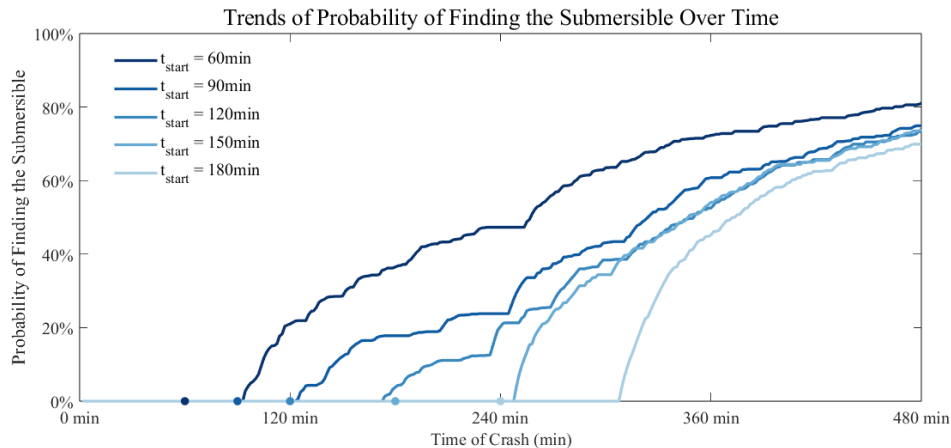
Figure 26 Trend of Probability Over Time with Ways to Reduce Uncertainty

Figure 26 shows the trends of probability over time in situation with ways to reduce uncertainty. It can be seen that the earlier AUV sets off, the probability of successful search and rescue will increase slightly, increasing from 75% to 80%.

The sensitivity analysis reflects that when a submersible accident may occur, we need to **seize the golden window period of search and rescue** as much as possible to increase the probability of searching success. What's more, it is also important to **take proper measures to reduce the uncertainty of submersible position**.

9   Evaluation and Promotion

9.1 Strengths And Weaknesses

Strengths:

- Based on historical data, the model adopts an objective approach to correct relevant parameters, such as the speed and direction of ocean currents, and takes into account certain errors, so as to achieve higher accuracy and authenticity.

- In the evaluation of search and rescue equipment, the subjective judgment and objective conditions are combined, and TOPSIS and AHP evaluation model are comprehensively used to make the model more reasonable and credible.

- AUV (Autonomous Underwater Vehicle) is creatively used to develop the search scheme, which gives full play to its high flexibility and high precision, making the model more contemporary and exploratory.

- The complexity of our model is low and the result of prediction position and planning search path is obtained quickly, so that the response can be rapid in the face of emergency.

Weaknesses:

- The conditions considered in the model are relatively ideal. Some influencing factors, such as possible vortices and sea water density faults, are ignored.

9.2 Possible Improvements

- Add more specialized correction factors, such as fluid dynamics analysis.

- Use a variety of search and rescue tools comprehensively, such as scanning sonar and professional data acquisition equipment, so that positioning and search and rescue more efficient.

Reference

[1] https://www.hycom.org/dataserver/gofs-3pt1/analysis

[2] https://hurricanescience.org/science/basic/water/index.html

[3] https://www.gebco.net/data_and_products

[4] Frank J. Millero, Alain Poisson, International one-atmosphere equation of state of seawater,

Deep-sea Research Part A. Oceanographic Research Papers, Volume 28, Issue 6,1981, P625-629.

[5] https://pic.ntimg.cn/file/20220331/31306436_152125108101_2.jpg

[6] https://img.redocn.com/sheji/20210406/yuanchuangshouhuixiaoqingxinxieshikatongburuleis

hen gwuhujingchahua_11428933.jpg.400.jpg

[7] https://www.geomar.de/en/news/article/poseidon-forscht-zukuenftig-unter-wasser

Memo